SCIENTIFIC REPORTS

OPEN

G6PDH activity highlights the operation of the cyclic electron flow around PSI in *Physcomitrella patens* during salt stress

Received: 17 July 2015
Accepted: 07 January 2016
Published: 18 February 2016

Shan Gao[1,2,*], Zhenbing Zheng[1,2,3,*], Li Huan[1,2] & Guangce Wang[1,2]

Photosynthetic performances and glucose-6-phosphate dehydrogenase (G6PDH) activity in *Physcomitrella patens* changed greatly during salt stress and recovery. In *P. patens*, the cyclic electron flow around photosystem (PS) I was much more tolerant to high salt stress than PSII. After high salt stress, the PSII activity recovered much more slowly than that of PSI, which was rapidly restored to pretreatment levels even as PSII was almost inactivate. This result suggested that after salt stress the recovery of the cyclic electron flow around PSI was independent of PSII activity. In addition, G6PDH activity and NADPH content increased under high salt stress. When G6PDH activity was inhibited by glucosamine (Glucm, a G6PDH inhibitor), the cyclic electron flow around PSI and the NADPH content decreased significantly. Additionally, after recovery in liquid medium containing Glucm, the PSI activity was much lower than in liquid medium without Glucm. These results suggested the PSI activity was affected significantly by G6PDH activity and the NADPH content. Based on the above results, we propose that G6PDH in *P. patens* has a close relationship with the photosynthetic process, possibly providing NADPH for the operation of the cyclic electron flow around PSI during salt stress and promoting the restoration of PSI.

The moss *Physcomitrella patens* has a relatively simple morphology, and its gametophyte is dominant in the life cycle. Moreover, it is a multicellular eukaryote that demonstrates a high rate of homologous recombination[1]. These advantages make it an ideal model for the analysis of most aspects of plant biology. More importantly, *P. patens* is highly tolerant to a variety of stresses, such as cold, drought and high salt[2–6]. As a result, it has been used in investigating the responses of plants to abiotic stresses.

The abiotic stresses, such as drought and high salt, profoundly affect the physiological functions of plants[7,8]. In fact, a number of physiological processes, including photosynthesis and carbohydrate metabolisms, are sensitive to abiotic stresses. Photosynthesis, and especially photosynthetic electron flow, is a sensitive sensor for different stresses, which not only provides energy but also represents the reception of environmental information[9–11]. Many studies have reported that photosynthetic electron flow, particularly the cyclic electron flow around PSI, plays a significant physiological role in plant responses to stresses, which could provide ATP and protect photosynthetic apparatus under stress conditions[12–17]. In addition, during re-hydration, the recovery of PSI in desiccated macro-algae was much faster than that of PSII, and could still be restored when PSII was suppressed[18,19]. This introduces the issue of the source of the electrons involved in the cyclic electron flow around PSI during recovery when PSII is inhibited.

When plants are subjected to stresses, not only does the photosynthetic process change significantly, but also the carbohydrate metabolism, particularly the oxidative pentose-phosphate pathway (OPPP), demonstrates a positive response to stresses. Glucose-6-phosphate dehydrogenase (G6PDH), which catalyzes the first step of the OPPP and regulates NADPH provision in plants, is a key enzyme of the OPPP. The activity and content of G6PDH rise remarkably in stressed plants[20–23]. NADPH is an important molecule in the redox balance of plant

[1]Key Laboratory of Experimental Marine Biology, Institute of Oceanology, Chinese Academy of Sciences, Qingdao 266071, China. [2]Laboratory for Marine Biology and Biotechnology, Qingdao National Laboratory for Marine Science and Technology, Qingdao, China. [3]University of Chinese Academy of Sciences, Beijing, 100049, China. *These authors contributed equally to this work. Correspondence and requests for materials should be addressed to G.W. (email: gcwang@qdio.ac.cn)

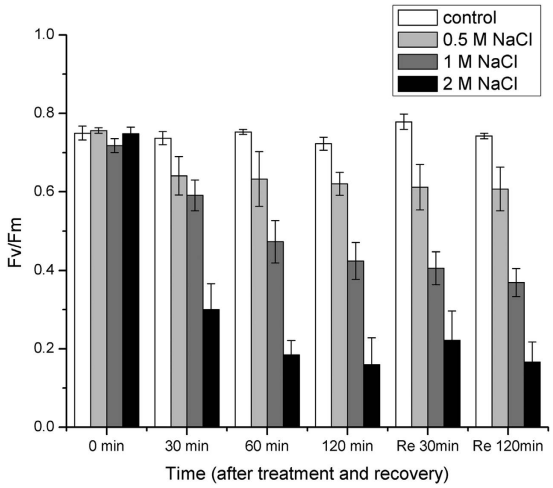

Figure 1. Changes in F_v/F_m in *P. patens* during treatments with control (normal liquid medium), 0.5 M, 1 M and 2 M NaCl solutions and after recovering in normal liquid medium. Re is the abbreviation of recovery. Data shown are the means of five independent experiments (±SD).

cells and is also required for plant protection against oxidative damage because many environmental conditions induce oxidative stress. In addition, NADPH can donate electrons to the photosynthetic electron flow[12,24]. This also raises the question of whether the OPPP provides NADPH for the operation of the cyclic electron flow around PSI during recovery.

The aim of this work was to study the responses of the photosynthetic electron flow and G6PDH in *P. patens* to high salt stress and the physiological link between the two processes. Particular attention was paid to the restoration of PSI and PSII during recovery and the responses of G6PDH activity and NADPH content to salt stress. The data obtained demonstrate that G6PDH has a close relationship with the photosynthetic process and might provide NADPH for the operation of the photosynthetic electron flow and the promotion of PSI restoration.

Results

The photosynthetic activities of gametophores in response to salt stress. Salt stress has great impact on the photosynthetic activities of the gametophores (Figs 1 and 2, and Supplementary Figure S1). The maximum quantum yield (F_v/F_m) decreased slightly during the course of the 0.5 M NaCl treatments in comparison with the control. After recovering in liquid medium for 30 min and 120 min, the F_v/F_m did not change significantly. In contrast, when the salinity increased (1 M and 2 M NaCl), F_v/F_m declined significantly and remained at a low level during recovery (Fig. 1). In comparison with the control (Fig. 2A), the activities of PSII and PSI decreased gradually during 0.5 M NaCl treatments, as suggested by the ETRII and ETRI. After recovery, both PSII and PSI could be restored (Fig. 2B). During the high salt treatments (1 M and 2 M NaCl), the PSII activity declined dramatically and could not be restored after 120 min of recovery. After 30 min of treatment with high salt solution, the PSI activity decreased significantly; however, with more prolonged treatments, the PSI activity did not change and was maintained at a low level (Fig. 2C,D). More importantly, after 30 min of recovery in liquid medium, even though the PSII activity was not restored, the PSI activity was rapidly restored, and after 120 min of recovery, it was almost restored to the pretreatment level. This phenomenon was much clearer in the gametophores treated with 2 M NaCl (Fig. 2D) than those treated with 1 M NaCl (Fig. 2C). The results suggested that the PSI in the gametophores of *P. patens* demonstrated a higher degree of tolerance to high salt stress than PSII and after treatments with high salt solution, the recovery of PSI activity was independent of the recovery of PSII activity.

Effects of G6PDH activity on the recovery of photosynthetic performance. The PSII and PSI activities during the course of high salt stress (2 M NaCl) were affected significantly by different inhibitors (Fig. 3). Glucm could effectively inhibit the G6PDH activity, which is the key enzyme that catalyzes the first step of the OPPP to produce NADPH. When the high salt solution contained Glucm, the PSI activity decreased significantly ($p < 0.05$), especially with prolonged treatment (Fig.3B). More importantly, after recovery in liquid medium containing Glucm, the ETRI (around 7) was much lower than the ETRI in liquid medium without Glucm (around 16) (Fig. 2D), suggesting that the PSI activity was affected significantly by the G6PDH activity. Meanwhile, the ETRII declined slightly in comparison with ETRII in the no Glucm condition. In contrast, when the high salt solution contained DCMU (a PSII inhibitor), both ETRI and ETRII decreased significantly ($p < 0.05$)(Fig. 3C). After recovering in liquid medium containing DCMU, ETRI was even lower than in the gametophores treated with Glucm. Furthermore, when the gametophores were treated with a high salt solution containing the two inhibitors (Fig. 3D), ETRII and especially ETRI decreased to very low levels. These results suggested that PSII and G6PDH activities during the course of high salt stress play important roles in the recovery of PSI activity.

We further determined the G6PDH activity and the NADPH content of the gametophores during the course of high salt stress. As Fig. 4 shows, the G6PDH activity was enhanced by the high salt stress. After 120 min of treatment, the G6PDH activity increased to the highest level (Fig. 4A). Nonetheless, during recovery, the G6PDH

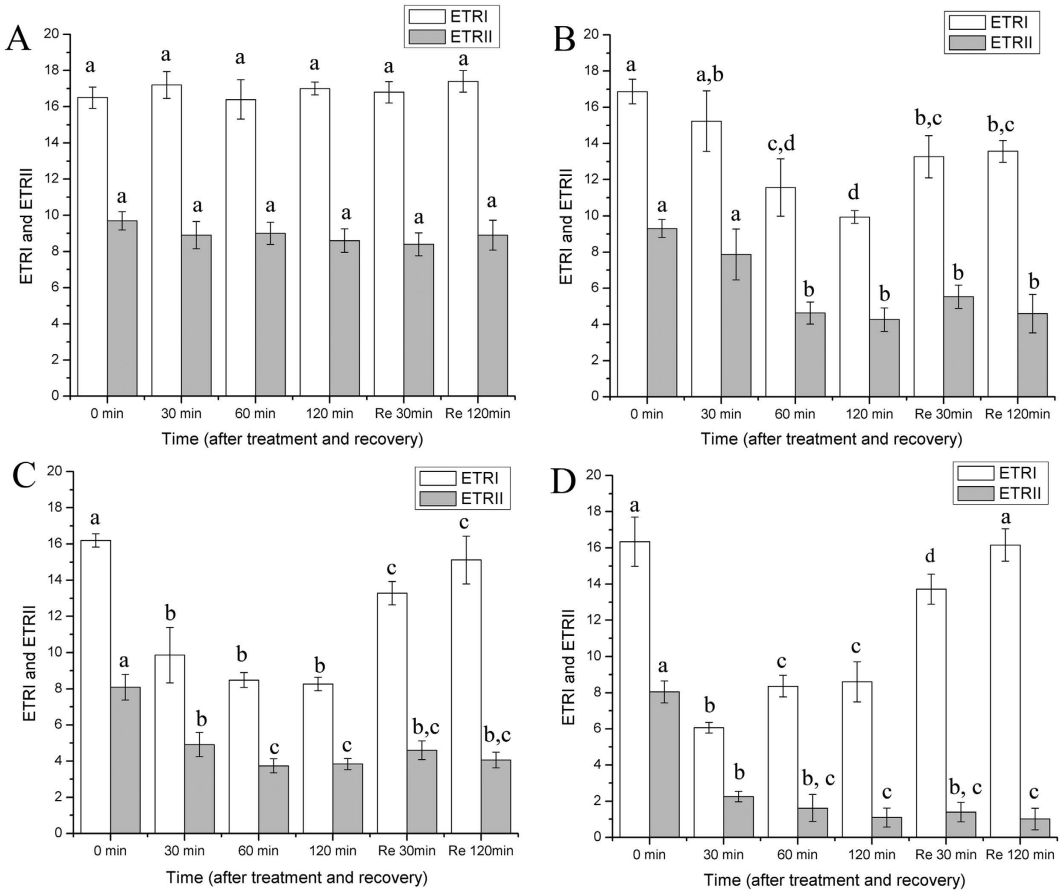

Figure 2. Variations in ETRII and ETRI in *P. patens* during treatments with control (normal liquid medium) (A), 0.5 M (B), 1 M (C) and 2 M (D) NaCl solutions and after recovering in normal liquid medium. Re is the abbreviation of recovery. Different letters represent significant differences between different times of salt treatment ($p < 0.05$, ANOVA, followed by Tukey's post-hoc test for comparisons, $\alpha = 0.05$). Data shown are the means of five independent experiments (±SD).

activity declined significantly ($p < 0.05$) and was maintained at a lower level. Meanwhile, the NADPH content increased greatly during the high salt treatment and rose to its highest value after 120 min of treatment, which was consistent with the G6PDH activity during high salt stress. In addition, when Glucm was present in the high salt solution, the G6PDH activity was inhibited greatly (Fig. 4A). During recovery in the liquid medium containing Glucm, the G6PDH activity was much lower than when in medium without Glucm. Moreover, the NADPH content decreased significantly ($p < 0.05$) with a prolonged treatment in the high salt solution containing Glucm, which was consistent with the G6PDH activity. These results further demonstrated that the G6PDH activity greatly affected the photosynthetic electron flow during high salt stress and especially the recovery of PSI activity.

Changes in PRK activity and RNA content during high salt stress. PRK, an enzyme involved in the Calvin cycle, decreased gradually during the course of the high salt stress. After 120 min of recovery, its activity had increased greatly. Moreover, during the high salt stress, there was a slight increase in the PRK activity in the presence of the G6PDH inhibitor (Glucm), although this was not significant (Fig. 5A). Additionally, after 120 min of treatment with the high salt solution, the RNA content increased significantly ($p < 0.05$). After recovery, the RNA content decreased dramatically. In the presence of Glucm, there was a small decrease during the course of the high salt treatment (Fig. 5B, Supplementary Figure S2).

Starch and soluble sugar responses to salt stress. Our results suggested that high salt stress greatly affects the starch and soluble sugar contents in the gametophores. The starch content decreased significantly ($p < 0.05$) during the course of the high salt treatment (Fig. 6A). When the gametophores recovered, the starch content increased dramatically. Moreover, Glucm barely affected the starch content of gametophores during high salt stress and recovery. Meanwhile, the soluble sugar content decreased significantly ($p < 0.05$) during the course of the high salt stress. After recovery, its content did not change significantly. In addition, Glucm had small effects on the soluble sugar content of the gametophores during high salt stress and recovery. In particular, after 30 min of recovery in the presence of Glucm, the sugar content declined significantly ($p < 0.05$) (Fig. 6B).

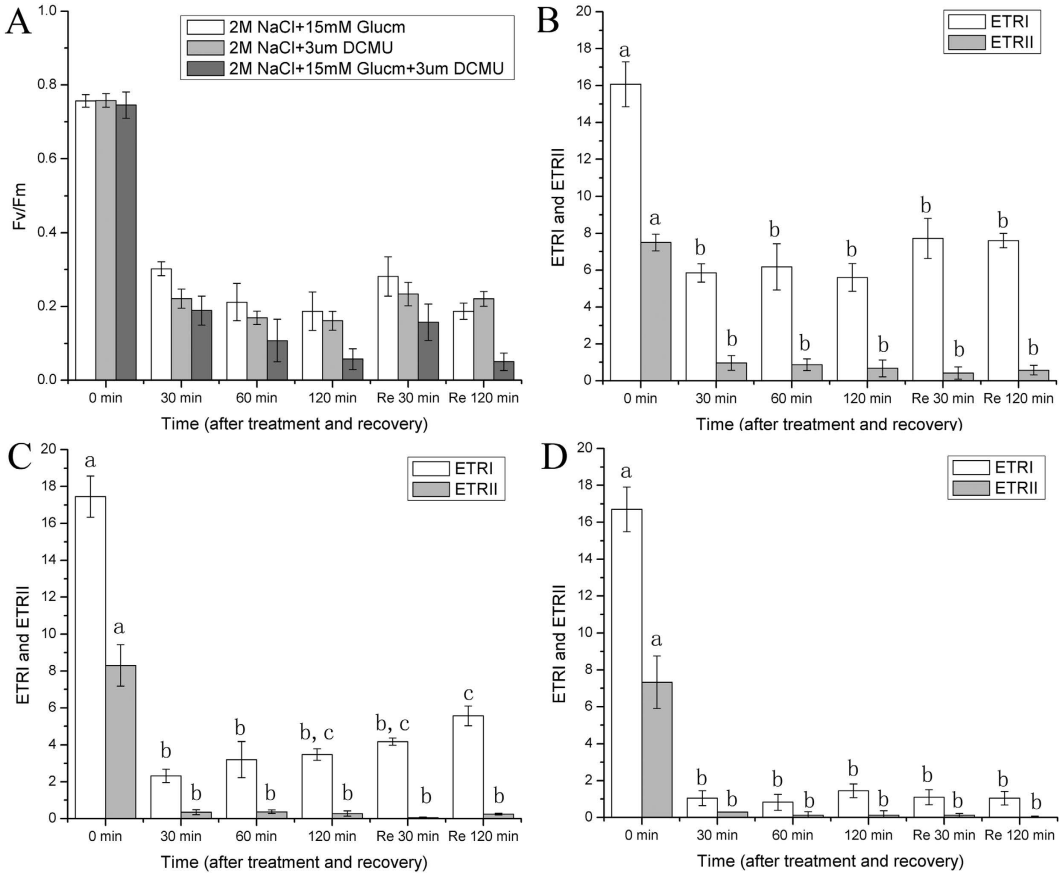

Figure 3. Responses of F_v/F_m, ETRII and ETRI in *P. patens* to 2 M NaCl solution containing DCMU and Glucm. (**A**) Changes in F_v/F_m in *P. patens* during immersion in 2 M NaCl solutions which contained 15 mM Glucm, 3 uM DCMU and the two inhibitors, respectively; Responses of ETRII and ETRI in *P. patens* during immersion in 2 M NaCl solution to 15 mM Glucm (**B**), 3 uM DCMU (**C**) and the two inhibitors (**D**). Re 30 min and Re 120 min means that the gametophores were restored in liquid medium containing the same inhibitor as they were treated with 2 M NaCl solutions. Different letters represent significant differences between different times of salt treatment ($p < 0.05$, ANOVA, followed by Tukey's post-hoc test for comparisons, $\alpha = 0.05$). Data shown are the means of five independent experiments ($\pm$SD).

Discussions

It is known that F_v/F_m is a sensitive indicator of the photosynthetic performance of plants and decreases when plants are subjected to stresses[25]. Our results showed that F_v/F_m declined substantially during salt stress (Fig. 1), demonstrating that the photosynthetic performance of *P. patens* was affected greatly by salt stress. During high salt treatment, ETRII decreased to a very low level (almost to 0) whereas the ETRI value remained high, suggesting that the PSI in *P. patens* was much more tolerant to salt stress than the PSII. In fact, similar phenomena occur in other drought-tolerant plants and algae, such as *Paraboea rufescens*, *Ulva prolifera* and *Porphyra yezoensis*[16,18,19]. Actually, both salt stress and drought could induce dehydration (osmotic stress) of plants, but salt stress also comprises ionic stress since the inevitable uptake or loss of ions will cause ionic stress to plants. Therefore, although the PSI in plants demonstrated much more tolerant to drought and salt stress, the response mechanisms to the two different stresses may be different[5,8]. In particular, the recovery of the PSI activity was much faster than that of PSII (Fig. 2B,C,D). Moreover, when PSII was inhibited by DCMU, PSI could still be restored, indicating that the recovery of the cyclic electron flow around PSI was independent of PSII activity after salt stress. It has been reported that in some intertidal macro-algae, after recovering from stresses, even though the linear electron flow was suppressed by DCMU, the cyclic electron flow around PSI could still be restored[18,23]. Based on the above results and the published data, we hypothesized that there may be other electron sources (in addition to electrons from water oxidation at PSII) that could donate electrons to PSI under salt stress and especially during recovery.

Many studies have reported that G6PDH plays an important role in the adaptation to a variety of stresses, such as salt stress and drought[20,22,26]. Under salt stress or drought conditions, the G6PDH activity in soybean roots was greatly enhanced, which modulated redox homeostasis under environmental stresses [21,27]. Both the G6PDH activity and the NADPH content in the stress-tolerant green macro-algae *U. prolifera* increased significantly during salt stress [23]. In addition, Rai, *et al.*[28] reported that the NADPH level was induced in *Anabaena* cells under salt stress, and the induction of NADPH and transketolase indicated OPPP's operation during salt stress. In fact, G6PDH is the key regulatory enzyme of the OPPP, which controls the flow of carbon and produces NADPH to

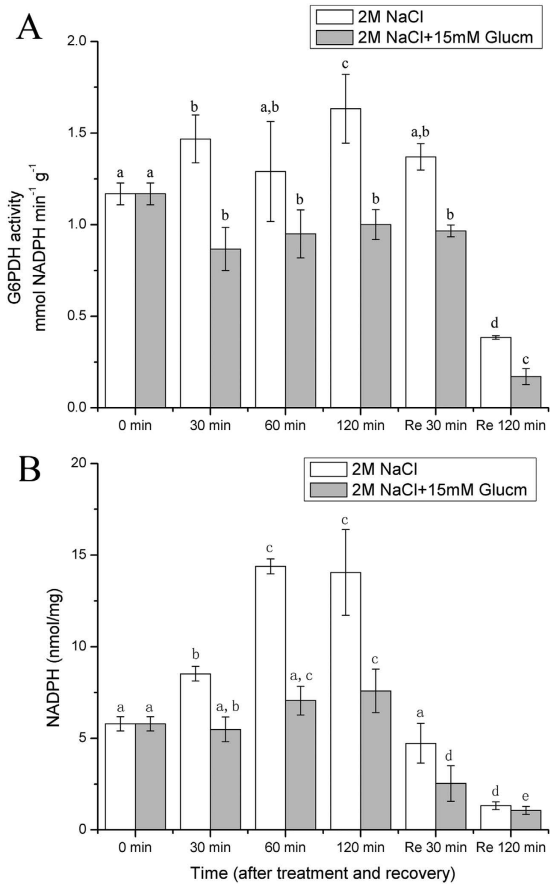

Figure 4. Effects of 2 M NaCl solution on G6PDH activity and NADPH content in *P. patens* and responses of G6PDH and NADPH to 15 mM Glucm. Re 30 min and Re 120 min means that the gametophores were restored in liquid medium. (**A**) G6PDH activity. (**B**) NADPH content. Different letters represent significant differences between different times of salt treatment ($p < 0.05$, ANOVA, followed by Tukey's post-hoc test for comparisons, $\alpha = 0.05$). Data shown are the means of five independent experiments ($\pm$SD).

meet the cellular needs of reductive biosynthesis[29]. Our results suggested that during the course of salt stress, the G6PDH activity in *P. patens* increased significantly ($p < 0.05$) (Fig. 4A), which was consistent with the changes in the NADPH levels (Fig. 4B). Moreover, the cyclic electron flow around PSI could still operate during salt stress and be restored rapidly after recovery from salt stress when PSII was inactivated. In addition, as G6PDH activity was obviously inhibited by Glucm (a G6PDH inhibitor)[27], both the cyclic electron flow around PSI and the NADPH content decreased significantly ($p < 0.05$), suggesting that there was a close relationship between them (Figs 3 and 4). In fact, NAD(P)H can donate electrons to photosynthetic electron carriers, which may have significant effects on the cyclic electron flow around PSI[24,30]. Based on our results and the published data, we proposed that the NADPH produced by G6PDH during the OPPP could provide electrons for the operation of the cyclic electron flow around PSI in *P. patens* during salt stress and recovery.

In addition to producing NADPH, the OPPP also provides R5P[31]. R5P not only participates in the Calvin cycle during the generation of ribulose 1,5-bisphosphate, but it can also be utilized for nucleotide synthesis[32]. The enzymes of the Calvin cycle are sensitive to stresses[33]. Furthermore, Huan, *et al.*[23] reported that the PRK activity of the Calvin cycle in *U. prolifera* declined greatly under high salt stress, which catalyzes the conversion of R5P to ribulose 1,5-bisphosphate. Our results suggested that the PRK activity in *P. patens* decreased significantly ($p < 0.05$)under salt stress (Fig. 5A). Moreover, the RNA content increased significantly ($p < 0.05$) under salt stress (Fig. 5B, Supplementary Figure S2). A plausible explanation is that the increase of G6PDH activity and the decrease of PRK activity resulted in an accumulation of pentose, which is likely to improve RNA synthesis. In fact, it has been proposed that the excess synthesis of total RNA might help the cells overcome stress and ready themselves for non-stressed conditions[23]. Thus, we suggested that the increased RNA content in *P. patens* during salt stress increases the moss' ability to survive salt stress.

In addition, the starch content in *P. patens* decreased significantly ($p < 0.05$) during salt stress, suggesting that salt stress accelerated starch degradation. In fact, a variety of stresses, including temperature and drought stress, could induce starch degradation[23,34,35,36]. Moreover, Johnson and Alric[24] proposed that the starch breakdown plays an important role in the donation of electrons to the photosynthetic cyclic electron flow around PSI in *Chlamydomonas reinhardtii*. In addition, our results indicated that the soluble sugar content in *P. patens* decreased significantly ($p < 0.05$) during salt stress, demonstrating decomposition. Based on our results and the

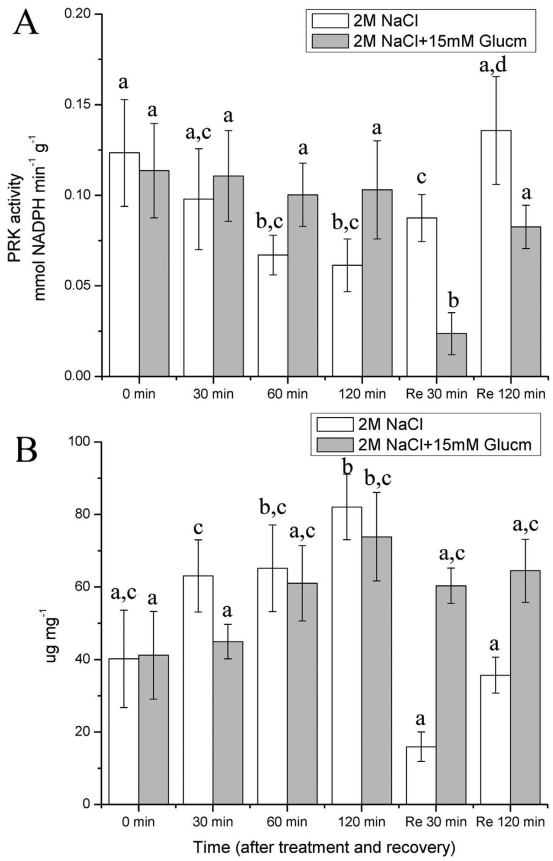

Figure 5. Effects of 2 M NaCl solution on PRK activity and RNA content in *P. patens* and responses of PRK and RNA to 15 mM Glucm. Re 30 min and Re 120 min means that the gametophores were restored in liquid medium. (**A**) PRK activity. (**B**) RNA content. Different letters represent significant differences between different times of salt treatment ($p < 0.05$, ANOVA, followed by Tukey's post-hoc test for comparisons, $\alpha = 0.05$). Data shown are the means of five independent experiments (±SD).

published data, we suggested that the increased starch degradation and G6PDH activity in *P. patens* during salt stress improved the generation of NADPH and pentose, which could donate electrons to the photosynthetic electron flow and be used during RNA synthesis, respectively.

Materials and Methods

Plant materials and growth conditions. *P. patens* ecotype 'Gransden 2004' (gift from professor Yikun He, Capital Normal University, China) was grown in BCD medium (1 mM $MgSO_4$, 10 mM KNO_3, 45 mM $FeSO_4$, 1.8 mM KH_2PO_4, pH 6.5) containing 0.5% (w/v) Glc and 0.75% (w/v) agar [4]. Gametophores were cultured at a light intensity of 60 μmol photons m^{-2} s^{-1} (16 h light/8 h dark). Four-week-old gametophores were used in the experiments.

Salt stress treatment and inhibitor treatment. Four-week-old gametophores were treated with control (normal liquid medium), 0.5 M, 1 M and 2 M NaCl for 2 h, respectively. During the course of these treatments, the photosynthetic activities of the gametophores were measured after 30, 60 and 120 min. For recovery, the gametophores were transferred into liquid medium. During recovery, the photosynthetic activities of the gametophores were measured after 30 and 120 min.

To investigate the effects of PSII and GAPDH on the PSI activity under salt stress, the inhibitors 3-(3′, 4′-dichlorophenyl)-1,1-dimethylurea (DCMU, a PSII inhibitor) and glucosamine (Glucm, a G6PDH inhibitor) were used in this study[19,27]. Four-week-old gametophores were treated with 2 M NaCl containing either 3 μm DCMU or 15 mM Glucm for 2 h. During treatment, the PSI and PSII activities were measured after 30, 60 and 120 min. Subsequently, the gametophores were transferred into liquid medium containing either 3 μm DCMU or 15 mM Glucm. After 30 and 120 min of recovery, the activities of PSI and PSII were measured. In addition, the activities of PSI and PSII were monitored under 2 M NaCl solution containing both 3 μm DCMU and 15 mM Glucm. Then, the gametophores were transferred into liquid medium containing both 3 μm DCMU and 15 mM Glucm for recovery. The activities of PSI and PSII were measured after 30 and 120 min of recovery.

Chlorophyll fluorescence and P700 measurement. As described previously[18], the chlorophyll fluorescence of PSII and the redox state of P700 (an indicator of PSI activity) of the gametophores were measured

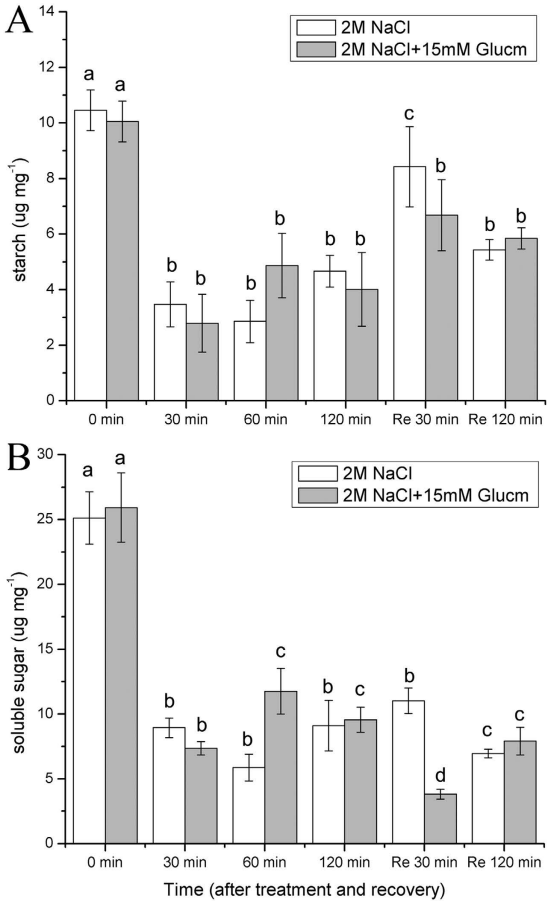

Figure 6. Effects of 2 M NaCl solution on starch and soluble sugar content in *P. patens* and responses of starch and soluble sugar levels to 15 mM Glucm. Re 30 min and Re 120 min means that the gametophores were restored in liquid medium. (**A**) starch content. (**B**) soluble sugar content. Different letters represent significant differences between different times of salt treatment ($p < 0.05$, ANOVA, followed by Tukey's post-hoc test for comparisons, $\alpha = 0.05$). Data shown are the means of five independent experiments ($\pm$SD).

concomitantly during high salt treatment using a Dual-PAM-100 fluorometer (Walz, Effeltrich, Germany) connected to a computer. Before measurement, the gametophores were dark-adapted for 10 min. F_0 (the minimum fluorescence) was determined and subsequently a saturating flash was applied to detect the maximal fluorescence (F_m). The difference between F_m and F_0 was referred to as the variable fluorescence (F_v), and the maximum quantum yield was obtained as F_v/F_m[37]. F_m' was detected as the gametophores were illuminated. The steady-state value of fluorescence immediately before the saturating flash is termed F_t. The effective photochemical quantum yield of PS II [Y(II)] is calculated as $(F_m' - F_t)/ F_m'$. It is assumed that photons are evenly distributed between PSI and PSII and an average of leaf absorbs about 84% of incident PAR (photosynthetically active radiation)[37,38]. Hence, in Dual-PAM-100 system, the following expression serves for the relative electron transport rate (ETR): $ETRII = 0.84 \times 0.5 \times PAR \times Y(II) = 0.42 \times PAR \times Y(II)$[37,38].

In analogy to chlorophyll fluorescence measurement, the saturation pulse method was used to determined the P700 parameters[39]. Although the measurement of P700 was often affected by plastocyanin (PC) signal when the excitation wavelength is 700 nm, but in Dual-PAM-100 system, P700 was measured in the dual-wavelength mode (difference of intensities of 875 and 830 nm pulse modulated measuring light reaching the photodetector)[39]. The PC signal still exists in Dual-PAM-100 system its effect on P700 measurement was very weak[40]. The maximal P700 signal, P_m, was determined by application of the saturation pulse in the presence of far-red light, which was defined in analogy to F_m. The zero P700 signal (P_0) was determined when complete reduction of P700 was induced after the saturation pulse and cessation of far-red illumination. The maximal P700 signal (P_m') was induced by combined actinic illumination with the saturation pulse. Based on P_m, P_0 and P_m', Y(I) was calculated automatically by Dual-PAM-100 software. Moreover, ETRI was calculated by Dual-PAM-100, which was defined in analogy to ETRII[41].

Determination of G6PDH and phosphate-5-ribulose kinase (PRK) activities. For the determination of G6PDH activity, an equal wet weight, 0.1 g, of gametophores selected at different times during the salt treatments was frozen in liquid nitrogen and ground into powder. Then, 300 μl extraction buffer, containing 50 mM Hepes-Tris (pH 7.8), 3 mM $MgCl_2$, 1 mM EDTA, 1 mM phenylmethylsulfonyl fluoride and 1 mM dithiothreitol, was added. Subsequently, the homogenate was centrifuged at 12,000 × *g* for 10 min at 4 °C. Subsequently,

10 μl of the extract was added to 390 μl assay buffer [50 mM Hepes-Tris (7.8), 3.3 mM $MgCl_2$, 0.5 mM D-glucose-6-phosphatedisodium salt and 0.5 mM $NADPNa_2$]. The reduction of $NADP^+$ to NADPH was determined as the changing rate of the 340 nm absorbance for the initial 5 min[27].

To determine the PRK activity of the gametophores at different times during the salt treatment, samples were ground in liquid nitrogen and an extraction buffer (100 mM HEPES-NaOH pH 8.0, 10 mM MgCl2, 0.4 mM EDTA, 1% polyvinylpyrrolidinone, 100 mM Na-ascorbate and 0.1% bovine serum albumin at 4 °C) was added. The enzymes initial activity was measured in a solution containing 30 mM HEPES-NaOH pH 8.0, 10 mM $MgCl_2$, 2 mM ATP, 2 mM phosphoenolpyruvate, 1 mM ribose 5-phosphate (R5P), 0.3 mM NADH, and 2 U ml^{-1} of lactate dehydrogenase, pyruvate kinase and ribose phosphate isomerase. The reaction was initiated by adding the extract's supernatant[42].

Determination of NADPH and RNA content. The NADPH content was determined according to Matsumura and Miyachi[43]. An equal wet weight of the gametophores were ground and then transferred to NaOH (0.1 M). The suspensions were kept at 100 °C for 2 min, then cooled to 0 °C and centrifuged (10,000 × *g*, 4 °C). NADPH was extracted into the supernatant obtained after the alkaline treatment. The alkaline extract was neutralized by adding an equivalent amount of HCl, followed by the addition of 0.1 ml of a solution containing 40 mM EDTA, 4.2 mM 3-(4,5-dimethylthiazolyl-2)-2,5-diphenyltetrazolium , 16.6 mM phenazine ethosulfate and 0.05 ml of G6P. After adjusting the total volume to 1 ml by adding H_2O, the test tubes were kept at 37 °C for 5 min. The reaction was started by adding 0.02 ml of G6P dehydrogenase. After the proper reaction time (30–60 min), the absorbency at 570 nm was measured. The concentration of NADPH in each extract was determined based on the standard curves.

The RNA contents of the gametophores with equal wet weight at different times during salt treatments were extracted using a Total RNA Kit (OMEGA), and the concentrations were measured using a NanoDrop 1000 Spectrophotometer (Thermo) and the purity of the isolated RNA from different conditions was determined through the electrophoresis (Supplementary Figure S2).

Analysis of starch and soluble sugar contents. The starch and soluble sugar contents were determined according to the methods described by Sánchez, *et al.*[44] and Brányiková, *et al.*[45], respectively, with minor modifications. An equal wet weight of the gametophores at different time during salt treatments were frozen in liquid nitrogen and ground into powder. Soluble sugar was extracted using 8 ml of 80% ethanol at 68 °C for 15 min and centrifuged (10,000 × *g*, room temperature). This step was repeated three times. The supernatants were combined and volatilized in an 85 °C water bath to a volume of 2–3 ml. Distilled water was then added to a final total volume of 10 ml. For the total hydrolysis of starch, 3.3 ml of 30% perchloric acid was added to the sediment, stirred for 15 min and centrifuged (10,000 × *g*, room temperature). This step was also repeated three times. The extracts were combined, and perchloric acid was then added to a final volume of 10 ml. Then, 0.1 ml of the soluble sugar and starch extracts were cooled to 0 °C, and 1 ml of 0.2% anthrone solution [0.2 g of anthrone in 100 ml of 72% (v/v) H_2SO_4] was added and blended quickly. The mixtures were kept in a water bath at 100 °C for 8 min, cooled to 20 °C, and the 625 nm absorbance levels were measured. A standard curve was created simultaneously using glucose. The soluble sugar contents were determined according to the calibration curve, while the starch contents were obtained by multiplying the measured values by 0.9.

Statistical analyses. The results were expressed as the mean values of five independent experiments ± standard deviation (SD). Data were used for statistical analysis via one-way analysis of variance (ANOVA) using the SPSS 18.0 statistical software. For the post-hoc analysis, Tukey test was used at an $\alpha = 0.05$ significance level.

References

1. Frank, W., Decker, E. & Reski, R. Molecular tools to study *Physcomitrella patens*. *Plant Biology* **7,** 220–227 (2005).
2. Wang, X. *et al.* Proteomic analysis of the response to high-salinity stress in *Physcomitrella patens*. *Planta* **228,** 167–177 (2008).
3. Wang, X. *et al.* Proteomic analysis of the cold stress response in the moss, *Physcomitrella patens*. *Proteomics* **9,** 4529–4538 (2009).
4. Wang, X. Q. *et al.* Exploring the mechanism of *Physcomitrella patens* desiccation tolerance through a proteomic strategy. *Plant Physiology* **149,** 1739–1750 (2009).
5. Cuming, A. C., Cho, S. H., Kamisugi, Y., Graham, H. & Quatrano, R. S. Microarray analysis of transcriptional responses to abscisic acid and osmotic, salt, and drought stress in the moss, *Physcomitrella patens*. *New Phytologist* **176,** 275–287 (2007).
6. Frank, W., Ratnadewi, D. & Reski, R. *Physcomitrella patens* is highly tolerant against drought, salt and osmotic stress. *Planta* **220,** 384–394 (2005).
7. Deinlein, U. *et al.* Plant salt-tolerance mechanisms. *Trends in Plant Science* **19,** 371–379 (2014).
8. Zhu, J. K. Salt and drought stress signal transduction in plants. *Annual Review of Plant Biology* **53,** 247 (2002).
9. Pfannschmidt, T. Chloroplast redox signals: how photosynthesis controls its own genes. *Trends in Plant Science* **8,** 33–41 (2003).
10. Anderson, J. M., Chow, W. S. & Park, Y.-I. The grand design of photosynthesis: acclimation of the photosynthetic apparatus to environmental cues. *Photosynthesis Research* **46,** 129–139 (1995).
11. Huner, N., Öquist, G. & Sarhan, F. Energy balance and acclimation to light and cold. *Trends in Plant Science* **3,** 224–230 (1998).
12. Shikanai, T. Cyclic electron transport around photosystem I: genetic approaches. *Annual Review of Plant Biology* **58,** 199–217 (2007).
13. Leister, D. & Shikanai, T. Complexities and protein complexes in the antimycin A-sensitive pathway of cyclic electron flow in plants. *Frontiers in plant science* **4** (2013).
14. Munekage, Y. *et al.* PGR5 is involved in cyclic electron flow around photosystem I and is essential for photoprotection in *Arabidopsis*. *Cell* **110,** 361–371 (2002).
15. Golding, A. J. & Johnson, G. N. Down-regulation of linear and activation of cyclic electron transport during drought. *Planta* **218,** 107–114 (2003).
16. Huang, W., Yang, S. J., Zhang, S. B., Zhang, J. L. & Cao, K. F. Cyclic electron flow plays an important role in photoprotection for the resurrection plant *Paraboea rufescens* under drought stress. *Planta* **235,** 819–828 (2012).
17. Kramer, D. M., Avenson, T. J. & Edwards, G. E. Dynamic flexibility in the light reactions of photosynthesis governed by both electron and proton transfer reactions. *Trends in Plant Science* **9,** 349–357 (2004).
18. Gao, S. & Wang, G. C. The enhancement of cyclic electron flow around photosystem I improves the recovery of severely desiccated *Porphyra yezoensis* (Bangiales, Rhodophyta). *Journal of Experimental Botany* **63,** 4349–4358 (2012).

19. Gao, S. *et al.* PSI-driven cyclic electron flow allows intertidal macro-algae *Ulva* sp.(Chlorophyta) to survive in desiccated conditions. *Plant and Cell Physiology* **52,** 885–893 (2011).
20. Scharte, J., Schon, H., Tjaden, Z., Weis, E. & Schaewen, A. V. Isoenzyme replacement of glucose-6-phosphate dehydrogenase in the cytosol improves stress tolerance in plants. *Proceedings of the National Academy of Sciences* **106,** 8061–8066 (2009).
21. Liu, Y. G., Wu, R. R., Wan, Q., Xie, G. Q. & Bi, Y. R. Glucose-6-phosphate dehydrogenase plays a pivotal role in nitric oxide-involved defense against oxidative stress under salt stress in red kidney bean roots. *Plant and Cell Physiology* **48,** 511–522 (2007).
22. Nemoto, Y. & Sasakuma, T. Specific expression of glucose-6-phosphate dehydrogenase (G6PDH) gene by salt stress in wheat (*Triticum aestivum* L.). *Plant Science* **158,** 53–60 (2000).
23. Huan, L. *et al.* Positive Correlation Between PSI Response and Oxidative Pentose Phosphate Pathway Activity During Salt Stress in an Intertidal Macroalga. *Plant and Cell Physiology* **55(8),** 1395–1403 (2014).
24. Johnson, X. & Alric, J. Interaction between starch breakdown, acetate assimilation, and photosynthetic cyclic electron flow in *Chlamydomonas reinhardtii*. *Journal of Biological Chemistry* **287,** 26445–26452 (2012).
25. Maxwell, K. & Johnson, G. N. Chlorophyll fluorescence—a practical guide. *Journal of Experimental Botany* **51,** 659–668 (2000).
26. Nee, G., Innocenti, G. & Issakidis-Bourguet, E. Redox regulation of root glucose-6-phosphate dehydrogenase by thioredoxins in the context of salt stress. *Journal of Biotechnology Computational Biology and Bionanotechnology* **94** (2013).
27. Liu, J., Wang, X. M., Hu, Y. F., Hu, W. & Bi, Y. R. Glucose-6-phosphate dehydrogenase plays a pivotal role in tolerance to drought stress in soybean roots. *Plant cell reports* **32,** 415–429 (2013).
28. Rai, S., Agrawal, C., Shrivastava, A. K., Singh, P. K. & Rai, L. Comparative proteomics unveils cross species variations in *Anabaena* under salt stress. *Journal of Proteomics* **98,** 254–270 (2014).
29. Schnarrenberger, C., Oeser, A. & Tolbert, N. Two isoenzymes each of glucose-6-phosphate dehydrogenase and 6-phosphogluconate dehydrogenase in spinach leaves. *Archives of Biochemistry and Biophysics* **154,** 438–448 (1973).
30. Bukhov, N. & Carpentier, R. Alternative photosystem I-driven electron transport routes: mechanisms and functions. *Photosynthesis Research* **82,** 17–33 (2004).
31. Porter, S. N., Howarth, G. S. & Butler, R. N. Non-steroidal anti-inflammatory drugs and apoptosis in the gastrointestinal tract: potential role of the pentose phosphate pathways. *European Journal of Pharmacology* **397,** 1–9 (2000).
32. Debnam, P. M. & Emes, M. J. Subcellular distribution of enzymes of the oxidative pentose phosphate pathway in root and leaf tissues. *Journal of Experimental Botany* **50,** 1653–1661 (1999).
33. Dias, M. & Bruggemann, W. Limitations of photosynthesis in *Phaseolus vulgaris* under drought stress: gas exchange, chlorophyll fluorescence and Calvin cycle enzymes. *Photosynthetica* **48,** 96–102 (2010).
34. Yang, J., Zhang, J., Wang, Z. & Zhu, Q. Activities of starch hydrolytic enzymes and sucrose-phosphate synthase in the stems of rice subjected to water stress during grain filling. *Journal of Experimental Botany* **52,** 2169–2179 (2001).
35. Kaplan, F. & Guy, C. L. β-Amylase induction and the protective role of maltose during temperature shock. *Plant Physiology* **135,** 1674–1684 (2004).
36. Murphy, M. S., Rao, Y. N. & Faldu, P. J. Invertase and total amylase activities in *Ulva lactuca* from different tidal levels under desiccation. *Botanica Marina* **31,** 53–56 (1988).
37. Schreiber, U. Pulse-Amplitude-Modulation (PAM) Fluorometry and Saturation Pulse Method: An Overview In *Chlorophyll Fluorescence: a Signature of Photosynthesis* (eds G.C. Papageorgiou & Govindjee) 279–319 (Springer, 2004).
38. Björkman, O. & Demmig, B. Photon yield of O2 evolution and chlorophyll fluorescence characteristics at 77 K among vascular plants of diverse origins. *Planta* **170,** 489–504 (1987).
39. Schreiber, U. & Klughammer, C. Saturation Pulse method for assessment of energy conversion in PS I. *PAM Application Notes* **1,** 11–14 (2008).
40. Dewez, D. & Perreault, F. Effect of the anthocyanic epidermal layer on Photosystem II and I energy dissipation processes in *Tradescantia pallida* (Rose) Hunt. *Acta Physiologiae Plantarum* **35,** 463–472 (2013).
41. Pfündel, E., Klughammer, C. & Schreiber, U. Monitoring the effects of reduced PSII antenna size on quantum yields of photosystems I and II using the Dual-PAM-100 measuring system. *PAM Application Notes* **1,** 21–24 (2008).
42. Rao, I. M. & Terry, N. Leaf phosphate status, photosynthesis, and carbon partitioning in sugar beet I. Changes in growth, gas exchange, and Calvin cycle enzymes. *Plant Physiology* **90,** 814–819 (1989).
43. Matsumura, H. & Miyachi, S. In *Methods in Enzymology* Vol. 69 (ed A. San Pietro) 465–470 (Academic Press, 1983).
44. Sánchez, F. J., Manzanares, M., de Andres, E. F., Tenorio, J. L. & Ayerbe, L. Turgor maintenance, osmotic adjustment and soluble sugar and proline accumulation in 49 pea cultivars in response to water stress. *Field crops research* **59,** 225–235 (1998).
45. Bránykiková, I. *et al.* Microalgae—novel highly efficient starch producers. *Biotechnology and Bioengineering* **108,** 766–776 (2011).

Acknowledgements

This work was supported by Laboratory for Marine Biology and Biotechnology, Qingdao National Laboratory for Marine Science and Technology (Qingdao, China); Promotive research fund for excellent young and middle-aged scientists of Shandong Province (BS2014HZ014); China postdoctoral Science Foundation on the 58th grant program (2015M580614); Strategic leading science and technology projects of Chinese Academy of Sciences(XDA11020404); National Natural Science Foundation of China (41376164).

Author Contributions

S.G. and Z.Z. carried out the experiments and wrote the main manuscript text. S.G., Z.Z., L.H. and G.W. prepared Figures 1–6. G. W. designed the experiment. All authors reviewed the manuscript.

Additional Information

Supplementary information accompanies this paper at http://www.nature.com/srep

Competing financial interests: The authors declare no competing financial interests.

How to cite this article: Gao, S. *et al.* G6PDH activity highlights the operation of the cyclic electron flow around PSI in *Physcomitrella patens* during salt stress. *Sci. Rep.* **6**, 21245; doi: 10.1038/srep21245 (2016).